

Monitoring Structural Changes of Proteins in an Ion Trap over ~10–200 ms: Unfolding Transitions in Cytochrome c Ions

Ethan R. Badman, Cherokee S. Hoaglund-Hyzer, and David E. Clemmer*

Department of Chemistry, Indiana University, Bloomington, Indiana 47405

A new technique for studying the time dependence of conformational changes of gas-phase protein ions is described. In this approach, a short pulse of electro-sprayed protein ions is introduced into an ion trap and stored. After a defined time period, the distribution of ions is ejected from the trap into an ion mobility/time-of-flight mass spectrometer. Combined measurements of mobilities and flight times in the mass spectrometer provide information about the abundances of different conformer types and charge-state distributions. By varying the storage time in the trap, it is possible to monitor changes in ion conformation that occur over extended time periods (~10–200 ms). The method is demonstrated by examining changes in cytochrome c ion conformations for the +7 to +10 charge states.

Measurements of the time scales associated with protein folding are challenging because of the vast range of times associated with assembling different types of structures ($\sim 10^{-8}$ – 10^3 s). With this in mind, many strategies have been employed to study folding kinetics, including the following: stopped-flow measurements, combined with spectroscopic^{1–3} and mass spectrometry (MS)⁴ detection methods; laser-temperature jump^{5,6} and other spectroscopic⁷ approaches for examining fast-folding processes; and isotopic exchange monitored by nuclear magnetic resonance⁸ and MS techniques.⁹

Recently, the structures and dynamics of protein ions have been investigated in the gas phase, where they can exist as isolated ions or be examined in the presence of a few water molecules.^{10,11} Several different techniques provide evidence that

the isolated ions undergo folding and unfolding transitions; in some ways, these transitions appear to resemble transitions that are observed in solution. Examination of the dynamic nature of polypeptide chains in the well-defined vacuum environment provides a means of assessing properties that are intrinsic to these molecules. However, as in solution, delineating the time scales associated with folding events presents a formidable experimental challenge.

Transitions that occur over times of seconds to minutes can be studied by trapping methods such as monitoring hydrogen/deuterium exchange levels by Fourier transform mass spectrometry (FTMS).^{12–17} Transitions that occur during ~0.5 to ~10 ms time scales have been followed by injected-ion mobility methods, which are sensitive to the average shapes of different conformations.^{18–20} To our knowledge, shorter time scale conformational changes (ns to μ s) have not been examined in detail for such large molecules in the gas phase. However, an intriguing microscopy experiment, involving the measurement of surface hillocks induced by high-energy collisions (hundreds of kiloelectronvolts) of protein ions with a surface, may provide information about structures at shorter times.^{21–24}

In this paper, we describe the initial development of a method that allows conformational changes that occur in the ~10–200-ms regime to be studied. In this approach, a short pulse of ions

- (1) Taniyama, Y.; Ogasahara, K.; Yutani, K.; Kikuchi, M. *J. Biol. Chem.* **1992**, *267*, 4619–4624.
- (2) Haezebrouck, P.; Noyelle, K.; Van Dael, H. *Biochemistry* **1998**, *37*, 6772–6780.
- (3) Noyelle, K.; Joniau, M.; Van Dael, H. *J. Mol. Biol.* **2001**, *308*, 807–819.
- (4) Kolakowski, B. M.; Konermann, L. *Anal. Biochem.* **2001**, *292*, 107–114.
- (5) Callender, R. H.; Dyer, R. B.; Gilman, R.; Woodruff, W. H. *Annu. Rev. Phys. Chem.* **1998**, *49*, 173–202.
- (6) Gruebele, M.; Sabelko, J.; Ballew, R.; Ervin, J. *Acc. Chem. Res.* **1998**, *31*, 699–707.
- (7) Gruebele, M. *Annu. Rev. Phys. Chem.* **1999**, *50*, 485–516.
- (8) Miranker, A.; Robinson, C. V.; Radford, S. E.; Aplin, R. T.; Dobson, C. M. *Science* **1993**, *262*, 896–900.
- (9) Green, M. K.; Lebrilla, C. B. *Mass Spectrom. Rev.* **1997**, *16*, 53–71.
- (10) Hoaglund-Hyzer, C. S.; Counterman, A. E.; Clemmer, D. E. *Chem. Rev.* **1999**, *99*, 3037–3079.
- (11) Jarrold, M. F. *Annu. Rev. Phys. Chem.* **2000**, *51*, 179–207.

- (12) Winger, B. E.; Lightwahl, K. J.; Rockwood, A. L.; Smith, R. D. *J. Am. Chem. Soc.* **1992**, *114*, 5897–5898.
- (13) Suckau, D.; Shi, Y.; Beu, S. C.; Senko, M. W.; Quinn, J. P.; Wampler, F. M.; McLafferty, F. W. *Proc. Natl. Acad. Sci. U.S.A.* **1993**, *90*, 790–793.
- (14) Wood, T. D.; Chorush, R. A.; Wampler, F. M.; Little, D. P.; Oconnor, P. B.; McLafferty, F. W. *Proc. Natl. Acad. Sci. U.S.A.* **1995**, *92*, 2451–2454.
- (15) Cassidy, C. J.; Carr, S. R. *J. Mass Spectrom.* **1996**, *31*, 247–254.
- (16) McLafferty, F. W.; Guan, Z. Q.; Haupts, U.; Wood, T. D.; Kelleher, N. L. *J. Am. Chem. Soc.* **1998**, *120*, 4732–4740.
- (17) Freitas, M. A.; Hendrickson, C. L.; Emmett, M. R.; Marshall, A. G. *Int. J. Mass Spectrom.* **1999**, *187*, 565–575.
- (18) Clemmer, D. E.; Hudgins, R. R.; Jarrold, M. F. *J. Am. Chem. Soc.* **1995**, *117*, 10141–10142.
- (19) Valentine, S. J.; Clemmer, D. E. *J. Am. Chem. Soc.* **1997**, *119*, 3558–3566.
- (20) Shelimov, K. B.; Clemmer, D. E.; Hudgins, R. R.; Jarrold, M. F. *J. Am. Chem. Soc.* **1997**, *119*, 2240–2248.
- (21) Quist, A. P.; Ahlbom, J.; Reimann, C. T.; Sundqvist, B. U. R. *Nucl. Instrum. Methods Phys. Res. Sect. B: Beam Interact. Mater. At.* **1994**, *88*, 164–169.
- (22) Reimann, C. T.; Quist, A. P.; Kopniczky, J.; Sundqvist, B. U. R.; Erlandsson, R.; Tengvall, P. *Nucl. Instrum. Methods Phys. Res. Sect. B: Beam Interact. Mater. At.* **1994**, *88*, 29–34.
- (23) Sullivan, P. A.; Axelsson, J.; Altmann, S.; Quist, A. P.; Sundqvist, B. U. R.; Reimann, C. T. *J. Am. Soc. Mass Spectrom.* **1996**, *7*, 329–341.
- (24) Reimann, C. T.; Sullivan, P. A.; Axelsson, J.; Quist, A. P.; Altmann, S.; Roepstorff, P.; Velazquez, I.; Tapia, O. *J. Am. Chem. Soc.* **1998**, *120*, 7608–7616.

is stored in an ion trap. After a defined time period, the ions are ejected from the trap and the structures of the different charge states are examined using a hybrid ion mobility/time-of-flight mass spectrometer. By varying the storage time in the trap, it is possible to accumulate detailed profiles of structural changes that occur over extended times. We demonstrate the method by examining conformations of different charge states of cytochrome *c*.

The cytochrome *c* system has been investigated extensively by isotopic exchange FTMS,^{13,14,16} measurements of collision cross section by scattering^{25–27} and ion mobility methods.^{18–20,28,29} The FTMS and ion mobility studies show evidence for multiple conformers within a charge-state family, and it is possible to induce structural transitions; however, direct comparison of structural information from these different techniques has been difficult—in part because of the vastly different time scales of the experiments. The results obtained in the present study (over the 10–200-ms time scale) provide a detailed look at an intermediate time scale and thus should help to link the shorter and longer time results. We find that the +7 to +10 charge states initially favor relatively compact forms. More elongated structures emerge after ~30–70 ms. In some charge states, there is evidence for at least two types of relatively compact conformers that have indistinguishable mobilities; additionally, it appears that we have identified some features that are associated with intermediates along the unfolding coordinate. After ~70 ms in the trap, the distribution of conformers does not appear to change significantly—even at the longest time (~200 ms) that we have studied. We speculate that these states persist and are the dominant species present in the longer time FTMS studies. It would also appear that the surface impact studies of this system are probing the more compact states that exist at shorter times.

The present data should also be relevant for studies of dissociation pathways in quadrupole ion traps. Recent collisional activation studies of hemoglobin,³⁰ insulin,³¹ and ubiquitin³² ions show that the fragmentation pathways depend strongly upon the charge state of the parent ion. The possible influence of parent ion conformation on fragmentation pathways is also currently of interest.^{33–37}

EXPERIMENTAL SECTION

General Information. The ion trap/ion mobility/time-of-flight approach used in these studies is described in detail elsewhere.^{38,39} A brief description of the experimental approach follows. Positively charged (protonated) ions are formed by atmospheric pressure electrospray of a solution containing horse heart cytochrome *c* (Sigma, >95% purity), ~10⁻⁵ M in 49:49:2 (volume %) water/methanol/acetic acid, into a 5-cm-long differentially pumped desolvation region that operates at a pressure of 1–10 Torr. Some ions exit the source through a 0.010-cm-diameter orifice and enter the main chamber of the instrument; a fraction of these is accumulated in an ion trap (RM Jordan, model C-1251) operated with a buffer gas pressure of ~10⁻³ Torr, of primarily helium buffer gas that comes from gas that exits the drift tube. Periodically, short packets of trapped ions are released and injected through a 0.08-cm-diameter orifice into a 50.6-cm-long drift tube. The drift tube is operated with ~2 Torr of 300 K He buffer gas and a uniform 12.85 V cm⁻¹ drift field. As ions drift through the gas, they are separated by differences in their mobilities (or collision cross sections), which depend on their shapes and charge state. Compact conformers have higher mobilities than more extended conformers. A small fraction of mobility-separated ions exits the drift tube and is focused into the source region of the time-of-flight mass spectrometer. Here, high-voltage, high-frequency pulses, synchronous with the initial injection pulse, are used to initiate time-of-flight measurements in the mass spectrometer. Because flight times in the evacuated flight tube are much shorter than drift times through the buffer gas, it is possible to record hundreds of mass spectra with respect to each packet of ions that is injected into the drift tube. In this manner, cross sections and charge-state distributions for distributions of ions can be measured in a single experimental sequence. We refer to this as a nested drift (flight) time measurement.⁴⁰

Pulse Sequence for Monitoring Changes in Conformation in the Trap. A key feature of the present experiment is the ability to store ions in the trap for a defined time prior to initiation of the ion mobility/time-of-flight experiment. To accomplish this, the synchronized pulsed sequence shown in Figure 1 is used. In this sequence, a deflector lens system gates ions into the ion trap. For these studies, this gate was 5 ms in duration; it is clear that there are advantages to utilizing substantially shorter gate times (for examining faster transitions) or longer times (for examining slow transitions or for improving the experimental duty cycle).⁴¹ After a variable trap delay (which ranged from 0 to 200 ms in these studies), ions are injected into the ion mobility instrument. Injection of ions into the drift tube initiates a synchronous pulse sequence at the back of the drift tube associated with the source of the time-of-flight mass spectrometer, as described previously.⁴⁰ The total drift (flight) time acquisition period that is covered by the pulse sequences used here was ~16.3 ms; thus, the 5-ms pulses of ions that are utilized in subsequent experiments can be introduced as the previous pulse of ions traverses the instrument.

(25) Cox, K. A.; Julian, R. K.; Cooks, R. G.; Kaiser, R. E. *J. Am. Soc. Mass Spectrom.* **1994**, *5*, 127–136.

(26) Covey, T.; Douglas, D. J. *J. Am. Soc. Mass Spectrom.* **1993**, *4*, 616–623.

(27) Chen, Y. L.; Collings, B. A.; Douglas, D. J. *J. Am. Soc. Mass Spectrom.* **1997**, *8*, 681–687.

(28) Woenckhaus, J.; Mao, Y.; Jarrold, M. F. *J. Phys. Chem. B* **1997**, *101*, 847–851.

(29) Mao, Y.; Woenckhaus, J.; Kolafa, J.; Ratner, M. A.; Jarrold, M. F. *J. Am. Chem. Soc.* **1999**, *121*, 2712–2721.

(30) Schaaff, T. G.; Cargile, B. J.; Stephenson, J. L.; McLuckey, S. A. *Anal. Chem.* **2000**, *72*, 899–907.

(31) Wells, J. M.; Stephenson, J. L.; McLuckey, S. A. *Int. J. Mass Spectrom.* **2000**, *203*, A1–A9.

(32) Reid, G. E.; Wu, J.; Chrisman, P. A.; Wells, J. M.; McLuckey, S. A. *Anal. Chem.* **2001**, *73*, 3274–3281.

(33) Wu, Q. Y.; Vanorden, S.; Cheng, X. H.; Bakhtiar, R.; Smith, R. D. *Anal. Chem.* **1995**, *67*, 2498–2509.

(34) Vachet, R. W.; Asam, M. R.; Glish, G. L. *J. Am. Chem. Soc.* **1996**, *118*, 6252–6256.

(35) Schnier, P. D.; Price, W. D.; Jockusch, R. A.; Williams, E. R. *J. Am. Chem. Soc.* **1996**, *118*, 7178–7189.

(36) Tsapralis, G.; Nair, H.; Somogyi, A.; Wysocki, V. H.; Zhong, W. Q.; Futrell, J. H.; Summerfield, S. G.; Gaskell, S. J. *J. Am. Chem. Soc.* **1999**, *121*, 5142–5154.

(37) Horn, D. M.; Breuker, K.; Frank, A. J.; McLafferty, F. W. *J. Am. Chem. Soc.*, submitted for publication.

(38) Hoaglund-Hyzer, C. S.; Clemmer, D. E. *Anal. Chem.* **2001**, *73*, 177–184.

(39) Henderson, S. C.; Valentine, S. J.; Counterman, A. E.; Clemmer, D. E. *Anal. Chem.* **1999**, *71*, 291–301.

(40) Hoaglund, C. S.; Valentine, S. J.; Sporleder, C. R.; Reilly, J. P.; Clemmer, D. E. *Anal. Chem.* **1998**, *70*, 2236–2242.

(41) Hoaglund, C. S.; Valentine, S. J.; Clemmer, D. E. *Anal. Chem.* **1997**, *69*, 4156–4161.

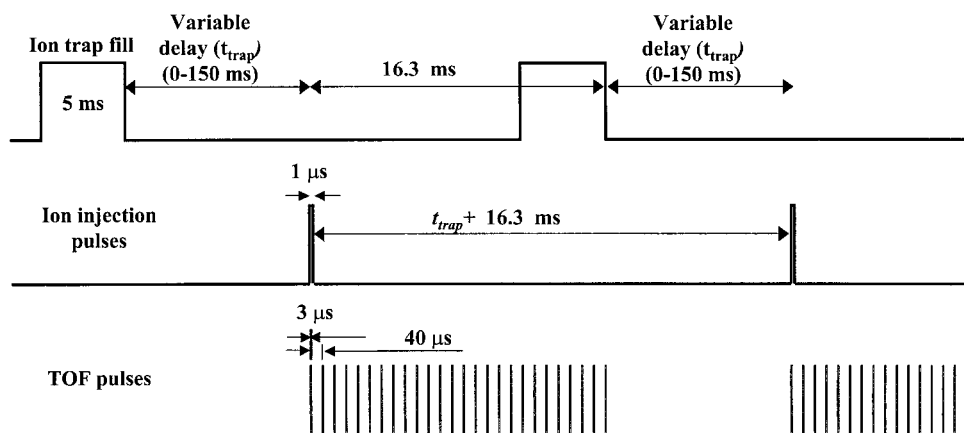


Figure 1. Experimental timing diagram showing variable delay time (t_{trap}) during which ions remain trapped in the quadrupole ion trap. The injection pulse of ions into the drift tube is initiated at a specified delay time from the end of the ion trap fill time. Time-of-flight acquisition pulses are synchronized with the drift pulse and occur at 40- μs intervals during the entire drift time measurement. See text for details.

Temperature of Stored Ions and Influence of Energy Used To Inject Ions into the Drift Tube. An important consideration regarding the time scales of structural changes is the temperature of the ions in the trap. The high-pressure electrospray source is expected to produce ions that are near the ambient laboratory temperature. To minimize collisional excitation of the ions prior to introduction in the trap, we utilize a low bias voltage ($\sim 3\text{--}5\text{ V}$) to focus the ions into the trap. The entrance and exit end caps and ring electrode of the trap are fixed to the same dc potential to minimize excitation along the axis of the beam. Thus, ions are expected to undergo a rapid collisional dampening process and then equilibrate to the helium buffer gas temperature (300 K in these studies).

Several experimental results suggest that collisional activation of ions upon injection and storage in the trap is minimal. Most importantly, as shown below, these experiments are extremely sensitive to compact conformations that have been previously shown to unfold upon collisional excitation.^{19,20} Additionally, changes in the source/trap bias over several volts do not influence the distribution of ions that is observed.

A factor that does influence the distribution of conformations is associated with the energy used to inject ions from the trap into the drift tube. Ions are ejected from the trap by turning off the rf trapping field and applying a short ejection pulse to the end cap. During ejection, as ions move past the end cap they are accelerated into the drift tube buffer gas. We define the injection voltage as the potential difference between the trap end cap and the drift tube entrance. As ions enter the drift tube, they are rapidly heated as their kinetic energy is thermalized by collisions with the buffer gas. Further collisions cool the ions to the buffer gas temperature. In the present studies, we have used the low injection voltage conditions (apparent voltages of $\sim 70\text{--}100\text{ V}$) that allow observation of compact conformers (which unfold at higher injection voltages). These conditions were chosen because they appear to minimize structural transitions that are induced upon injection into the drift tube; as shown below, at short trapping times, we are sensitive to an array of relatively unstable compact states. Studies have also been conducted at higher injection voltages (although the data are not described in detail here), and overall, the injection energy behavior is similar to results that have been reported previously.²⁰

Assignment of Conformation Types. Conformation types are assigned by comparison of the experimental ion mobility distributions with data recorded previously.^{20,42}

RESULTS AND DISCUSSION

Summary of Injected-Ion Mobility Measurements of the Collision Cross Sections for Different Charge States of Horse Heart Cytochrome *c*. Several experimental factors influence the types and abundances of conformations that are observed in injected-ion mobility studies of proteins. These include the electrospray solution and source conditions,⁴³ the energy used to inject ions into the drift tube,^{19,20,44,45} and the temperature of the buffer gas.²⁹ Below, we define five conformer types. These assignments are based on similarities in ion mobility peak shapes and trends observed across a range of charge states; it should be understood that many different structures (with similar cross sections) could comprise a peak that we refer to as a single conformer type.

A summary of different features for the cytochrome *c* system that have been observed many times over the past five years⁴² is given in Figure 2. In this plot, the solid symbols represent the positions of reproducible local maximums in the ion mobility distributions. The thin vertical lines connecting the various points represent the ranges associated with reproducible baseline signals (found under some of the experimental conditions). That is, under some conditions, the ion mobility data show evidence for other unresolved conformations (or evidence for structural transitions as ions drift through the instrument). The overall increase in cross section that is observed with increasing charge state has been explained previously by noting that an unfolding transition reduces repulsive Coulombic interactions.^{18–20,25,26}

Figure 2 includes cross sections (Ω) for several charge states that have not been reported previously in injected-ion mobility studies,^{18–20} including the following: $\Omega = 1420\text{ \AA}^2$ (+7); $\Omega = 1465$

(42) Clemmer, D. E.; Valentine, S. J.; Counterman, A. E.; Hoaglund-Hyzer, C. S.; Li, J. W.; Liu, Y., unpublished data.

(43) Li, J. W.; Taraszka, J. A.; Counterman, A. E.; Clemmer, D. E. *Int. J. Mass Spectrom.* **1999**, *187*, 37–47.

(44) Valentine, S. J.; Anderson, J. G.; Ellington, A. D.; Clemmer, D. E. *J. Phys. Chem. B* **1997**, *101*, 3891–3900.

(45) Valentine, S. J.; Counterman, A. E.; Clemmer, D. E. *J. Am. Soc. Mass Spectrom.* **1997**, *8*, 954–961.

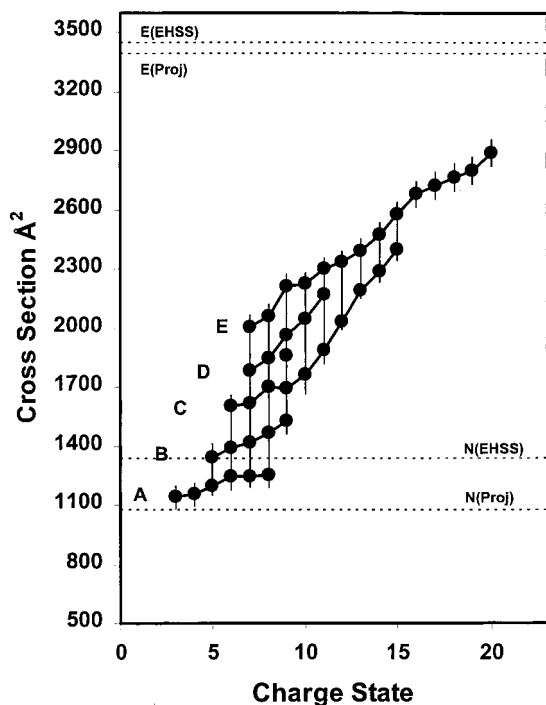


Figure 2. Plot of cross section versus charge state for cytochrome *c*. Conformation families are labeled A–E and described in more detail in the text. The dotted lines labeled N(Proj), N(EHSS), E(Proj), and E(EHSS) correspond to cross sections calculated using the projection method (Proj) and the exact hard-sphere scattering method (EHSS) for the native (N) and extended (E) conformations (see refs 19, 20). The EHSS⁴⁷ and projection⁴⁸ methods are described in more detail elsewhere.

Å^2 (+8); $\Omega = 1531, 1695, \text{ and } 1858 \text{ Å}^2$ (+9); $\Omega = 1762 \text{ and } 2050 \text{ Å}^2$ (+10); $\Omega = 1888 \text{ and } 2173 \text{ Å}^2$ (+11); $\Omega = 2034 \text{ Å}^2$ (+12); $\Omega = 2190 \text{ Å}^2$ (+13); $\Omega = 2287 \text{ Å}^2$ (+14); $\Omega = 2363 \text{ Å}^2$ (+15). These data can be grouped into five distinct conformer types. The most compact conformation (A) is observed for the +3 to +8 charge state. This conformer is favored for the +6, +7, and +8 charge states at low injection energies. Conformer type B is observed for the +5 to +9 charge states; this is the most compact structural type observed for +9 ions. Type C is observed for the +6 to +15 charge states; this conformer type appears as a peak that is substantially broader than other peaks within the same charge state—suggesting that a relatively wide range of different structures are grouped as type C. Conformer type D is observed for the +7 to +11 charge state, and the most extended conformers—type E ions—are observed for the +7 to +20 charge states.

Nested Drift(Flight) Time Data Sets Recorded at 29- and 75-ms Trapping Times. Figure 3 shows two-dimensional plots of nested drift(flight) time distributions recorded at trapping delay times of 29 and 75 ms. The ion signals observed in these experiments are also represented as mass spectra and ion mobility distributions, obtained by integrating the ion signals across the drift time and flight time dimensions, respectively. At both time delays, there is evidence for formation of the +7 through +15 charge states of cytochrome *c*, and the dominant peaks correspond to the +8 to +10 charge states. As the trapping time is extended, we note an overall decrease in total ion signal; ~50% of the ion signal is lost at our longest trapping times.

The primary difference between these data is associated with the very different distributions that are associated with the ion

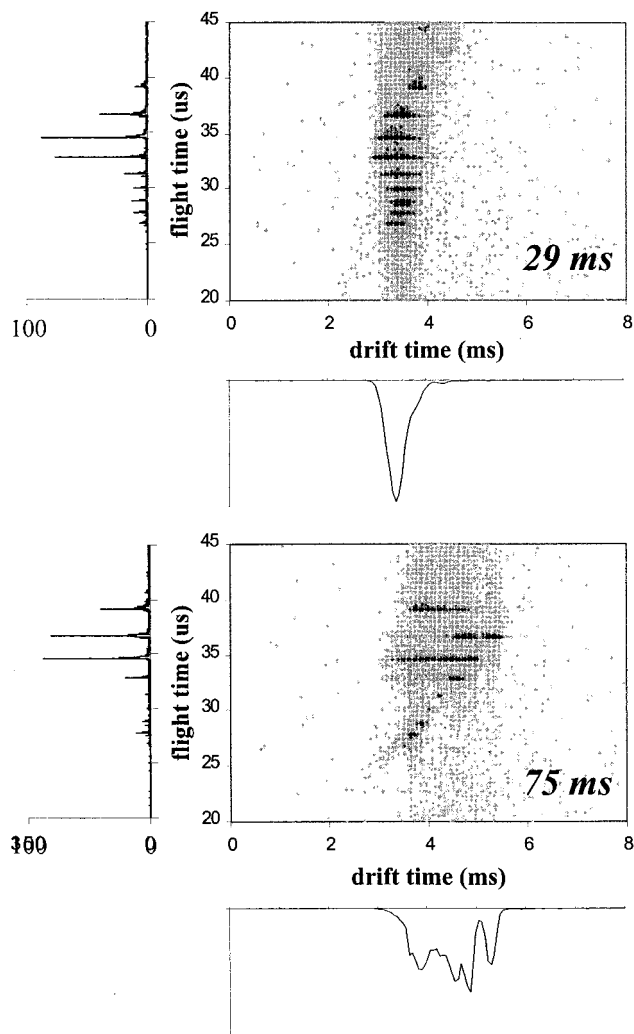


Figure 3. Nested drift(flight) time distributions showing the charge-state and conformational distributions of electrosprayed cytochrome *c* ions at t_{trap} delay times of 29 and 75 ms. Also shown are the summed mass spectrum and summed drift time spectrum for each ion trap delay time. The time-of-flight mass spectrum on the left of each plot was obtained by integrating the two-dimensional data over all drift times. The drift time distribution at the bottom of each plot was obtained by integrating the two-dimensional data over all flight times.

mobility experiment. At 29 ms, individual charge states exhibit peaks that are relatively broad [having full widths at half-maximums (fwhm) of ~0.2 to 0.5 ms]. Analysis of the peak positions indicates that the type A (+7 and +8), B (+9), and C (+10 to +15) conformations are present. The summed ion mobility distribution shows a single broad peak at ~3.5 ms; different charge states cannot be resolved based on differences in their mobilities.

At 75 ms, individual charge states exhibit evidence for multiple peaks. A visual comparison of the plots of the two-dimensional datasets taken at 29 and 75 ms shows that peaks in the drift time dimension, for the +10 to +15 charge states, are significantly narrower and appear at longer drift times. Thus, as the trapping time of these ions increases, it appears that many charge states have undergone unfolding transitions to produce new conformers—types B (+7), D (+8 and +9), and E (+8 to +15). This effect is so pronounced that new peaks appear in the integrated ion mobility distribution.

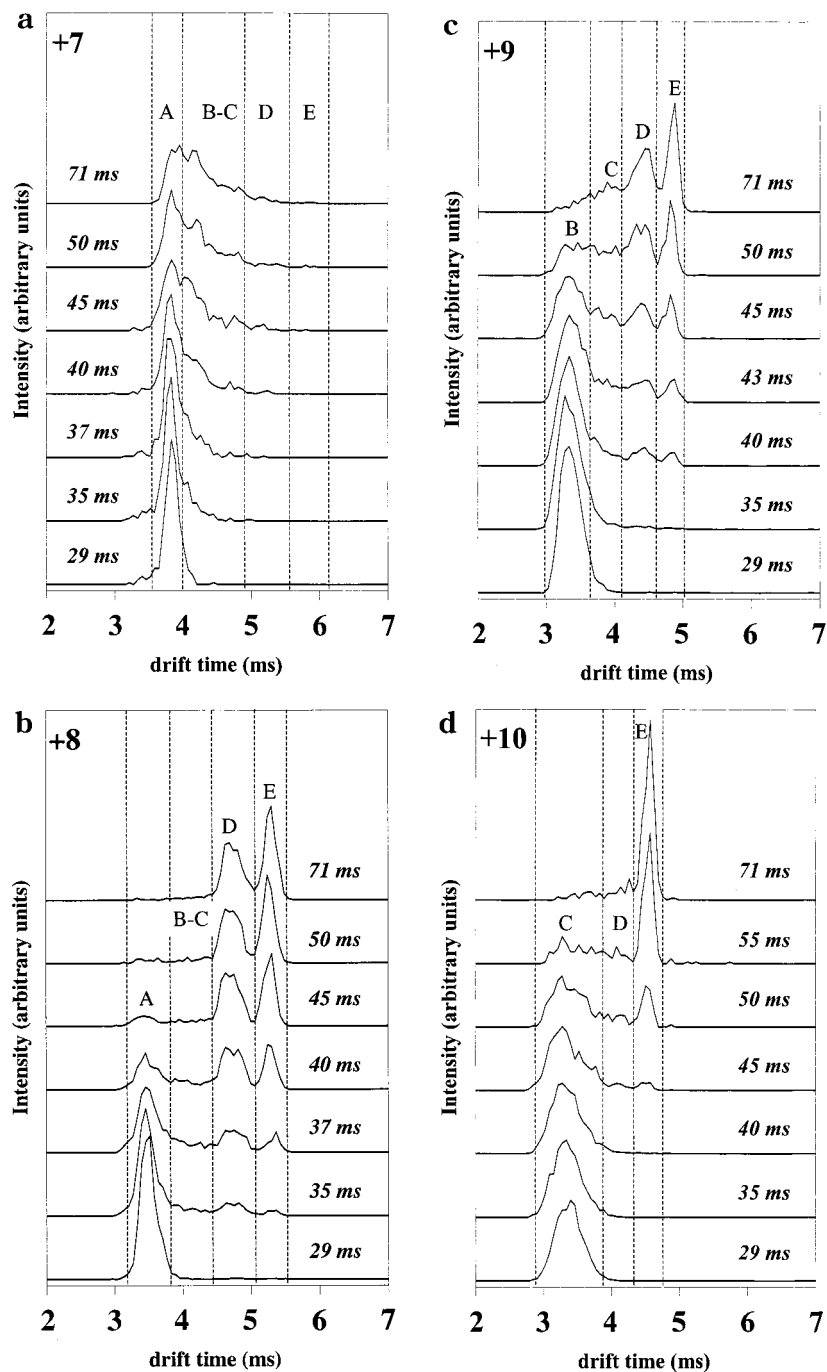


Figure 4. Drift time distributions for the +7 through +10 ions of cytochrome *c* at several t_{trap} delay times showing the transition from compact to extended ion conformations. The ion trap delay times for each state are denoted on the plot and were chosen to best represent the transitions observed for each charge state. The dotted lines show the drift time boundaries for each of the states.

Ion Mobility Distributions for Individual Charge States (+7 to +10) over a Range of Trapping Times. Additional information about the changes in structure that occur with trapping time can be obtained by examining the time dependence of ion mobility distributions for specific charge states. The most interesting transitions are observed for the +7 to +10 charge states; we focus our discussion on these ions.

Figure 4 shows ion mobility distributions for the +7 to +10 ions—obtained by taking slices across the drift(flight) time data sets at appropriate flight times. At short trapping times (~ 10 – 29 ms), +7 ions exist as compact A-type conformers. As the trapping time is extended beyond ~ 31 ms, the relative abundance of

compact A states decreases, and an unresolved feature shifted to longer drift times (consistent with B- and C-type conformers) appears. We note that it is interesting that only some of the +7 ions appear to unfold. The peak remains broad even at our longest trapping times—requiring that some of the +7 state remains as compact A-type conformers.

Ion mobility data for the +8 charge state also show that at short trapping times (< 29 ms) compact A-type ions are favored. As the trapping time increases, the fraction of the A state decreases. At 35 ms, a small unresolved tail from ~ 3.9 to 4.5 ms consistent with B- and C-type conformers is observed; additionally, small peaks corresponding to D and E conformers are present.

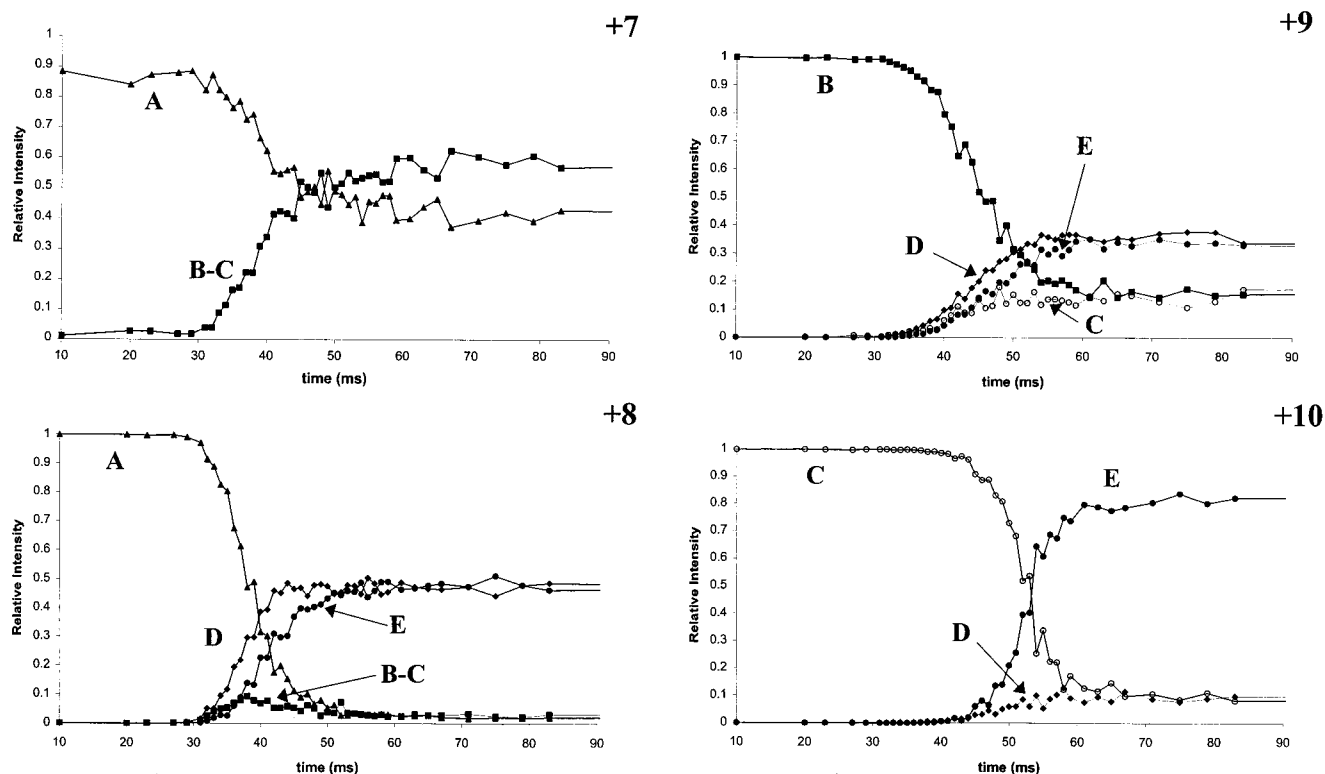


Figure 5. Plots showing the time dependence of relative ion intensity for each conformation of cytochrome *c* for the +7 to +10 charge states. The conformers for each charge state are labeled as described in Figure 3. Family A corresponds to solid triangles (\blacktriangle); family B, solid squares (\blacksquare); family C, open circles (\circ); family D, solid diamonds (\blacklozenge); family E, solid circles (\bullet). For the +7 and +8 charge states, the B and C conformers were not resolved and are labeled with solid squares (\blacksquare).

At longer times (>40 ms), the fractions of the A, and B, and C types decrease and the D and E conformers become the dominant states. By ~ 60 ms, the distribution of conformers appears to have stabilized and essentially remains constant to the longest trapping time, 200 ms.

The +9 ions initiate as type B ions (from 10- to 32-ms trapping time). As the trapping time increases, the population of the B state decreases and an array of C, D, and E structures are observed. Although the B state unfolds with time, a small fraction of B conformers persists to our longest trapping times.

The C state dominates the +10 ion population at short trapping times, and this state begins to unfold at ~ 38 ms. The unfolding process produces the D and E states; at trapping times in excess of ~ 50 ms, the E state dominates the distribution. It is noteworthy that at the longest trapping times the C ion does not entirely unfold, again showing that some of the compact ions do not unfold over the time scale examined.

Relative Population Changes of Conformers as a Function of Time. Figure 5 shows the populations of different conformer types as a function of trapping time. These plots are obtained by integrating the regions of the ion mobility data corresponding to each conformer type for ~ 40 data sets that were recorded over the transition region using incremental steps of 1.5 ms—creating a profile of structural changes that occur with time. A summary of threshold transition times and other information about conversion rates (discussed in more detail below) is provided in Table 1. It is instructive to describe the changes that are observed for each charge state. The +7(A) comprises essentially the entire ion

distribution until ~ 31 ms; at this time, a new feature that is not entirely resolved from the A state begins to appear (assigned as a combination of B and C states). At ~ 60 – 70 ms, the abundance of the A state appears to level off; $\sim 40\%$ of the +7 distribution remains as a compact A conformer—even at our longest trapping times (200 ms). The observation that $\sim 60\%$ of the +7(A) state ions rapidly convert into +7(B and C) conformers, while $\sim 40\%$ of the distribution does not increase in cross section (even at 200 ms) requires that there must be two types of compact A geometries; they are resolved here based on differences in the way that they unfold.

The time dependence of the +8(A) state is very different from that of the +7(A) data. For the +8 ions, the distribution of compact A state remains unchanged until ~ 29 ms. At this time there is a sharp increase in the abundance of the +8(D) conformer and a smaller increase in the +8(B and C) ions. Formation of the +8(E) state appears to be delayed by several milliseconds. From ~ 40 to 50 ms, the +8(D and E) states increase in abundance while the population of +8(A) precursor becomes vanishingly small. In this system, it is interesting that the +8(B and C) states decay within a few milliseconds of formation. This behavior indicates that at least some of the D and E states can be formed from the B and C states. That is, the B and C states are intermediates in the unfolding of at least some A conformers to D and E.

Still other behavior is exhibited by +9 ions. Here, the +9(B) state is observed at shortest trapping times (~ 10 – 32 ms); at longer times, the B state appears to give rise to the C, D, and E states. At ~ 70 ms, the B and C conformers each comprise $\sim 15\%$

Table 1. Measured Transition Times for Cytochrome *c* Ions Stored in an Ion Trap at 300 K

charge state	transition type	threshold time (ms) ^a	time required to reach midpoint (ms) ^b	rate of depletion of compact ion (s ⁻¹) ^c
+7	depletion of A	31	38.5	40
	formation of B/C	31	39	
+8	depletion of A	29	38	180
	formation of B/C	31	33.5	
	formation of D	29	37	
	formation of E	30	47	
+9	depletion of B	32	44.5	80
	formation of C	32	41	
	formation of D	32	44	
	formation of E	32	46	
+10	depletion of C	38	52.5	190
	formation of D	38	48	
	formation of E	40	53	

^a Time at which compact ion begins to unfold. Calculated by examining the first derivative of the plot of relative ion intensity versus time.

^b Time at which the relative ion intensity reaches 50% of the difference between the initial and final intensities. ^c Rates were obtained from the slope of the plot of the natural logarithm of the compact ion relative intensity versus time over the region where the compact ion unfolds. See text for details.

of the total; the D and E states each comprise ~35% of the distribution. The observation of a sharp decline of ~85% of the +9(B) ions combined with the result that a smaller fraction (~15%) persists to 200 ms indicates that there are at least two forms of B-type conformers.

The +10 charge state exhibits a relatively simple behavior. The +10(C) state is present initially. At ~38 ms, this state appears to evolve into the D and E states. At long times, the populations of the C, D, and E states are ~10, 10, and 80%. In this system, it appears that two types of +10(C) conformers are present—one that unfolds from ~40 to 50 ms, and another state that is stable to longer times.

Obtaining Semiquantitative Rate Data and Possible Explanations for an Experimental Induction Period. A striking feature of the data in Figure 5 is that compact states +7(A), +8(A), +9(B), and +10(C) appear to persist for substantial time periods (~30–40 ms) prior to the observation of a relatively rapid unfolding transition. We do not fully understand this induction period, and because of this, we present only a very limited analysis of the kinetics (which is best viewed as a semiquantitative measurement). Figure 6 shows a representative kinetic plot for the decrease in the population that was measured for the most compact ion +8(A). If we ignore the induction period, it is possible to fit the decay profile (over a range of ~33–50 ms) to obtain a unimolecular unfolding rate constant of 180 s⁻¹ (over this time scale). A similar semiquantitative analysis has been carried out for the decay profiles of the +7(A), +9(B), and +10(C) states; rate constants range from ~40 to 190 s⁻¹. These values are given in Table 1.

While we do not fully understand the induction period, it is interesting to consider possible origins for this behavior. One, of several possible explanations, that we are considering at this time is that this behavior is related to the distribution of internal ion temperatures that are initially present after the electrospray process. In order for this explanation to be consistent with the experimental result, ions would need to initially be colder than the ambient trap temperature. Solvent evaporation should cool the internal temperature of the protein ion. If the internal temperature falls below the ambient trap temperature (300 K),

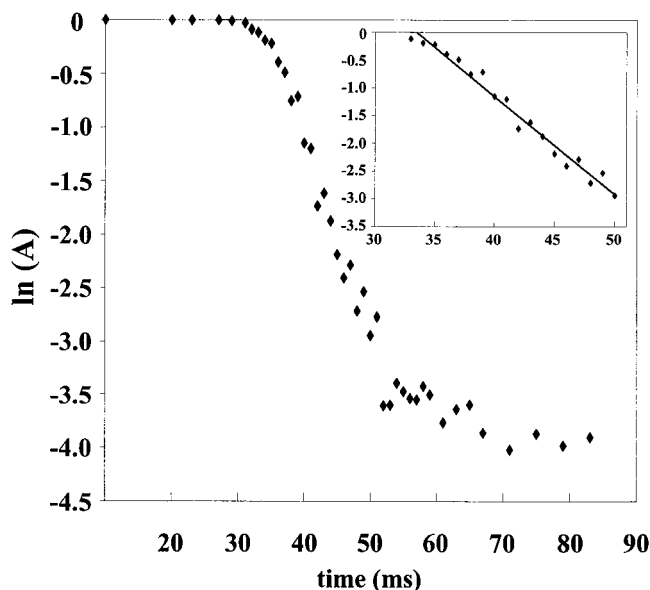


Figure 6. Plot of the natural logarithm of the relative intensity of the compact +8(A) ion of cytochrome *c* as a function of time. Inset: Linear least-squares fit of the data over the range of 33–50 ms.

ions would require some time to reach the trap temperature before the unfolding rate becomes significant. We are currently designing several experiments to test this idea.

SUMMARY AND CONCLUSIONS

A new approach for examining the dynamics of conformation changes in gas-phase protein ions has been described. In this approach, a short pulse of ions is introduced into an ion trap. These ions are then stored for a variable time period prior to examining the conformations of the distributions of charge states with a nested drift (flight) time approach. The approach makes it possible to examine time-dependent changes in conformations for distributions of ions from ~10 to 200 ms.

The method is demonstrated by examining the conformations of electrosprayed horse heart cytochrome *c* ions from 29 to 200 ms. Although the cytochrome *c* system has been examined in

detail by a number of techniques, the present results are the first to explore changes in conformation over this time scale and provide some interesting new information about several types of transitions. For example, it appears that the pathway for unfolding of the most compact A state depends heavily upon the charge state. Roughly 60% of the A state of the +7 ion unfolds to structures having cross sections that are consistent with the B and C states. These B and C ions appear to be stable for extended periods in the trap (~200 ms). The remaining 40% of the +7(A) state remains compact, signifying that the A state consists of two populations: one that can unfold, and one that remains compact. The +8(A) state abruptly unfolds to the B and C states as well as the more extended D and E conformers. In this charge state, we find evidence that the B and C states appear as intermediates along the unfolding pathway such that at least some of the D and E states are formed through the B and C states. There is no evidence for multiple A states for the +8 ion. The B state is favored for the +9 ion at short trapping times; at longer times, this state unfolds to the C, D, and E states. There appear to be two types of +9(B) ions; ~85% of the ions associated with the B peak unfold rapidly, while the remaining ions remain compact even at our longest trapping times. The ion mobility peak corresponding to the +10-

(C) state is dominant at short trapping times. About 90% of this state unfolds to the D and E states; another compact form (~10% of the distribution) does not appear to unfold.

We cannot resist the temptation to comment on the relationship of our results (at 200 ms) with the data obtained at longer times in quadrupole ion traps⁴⁶ (during collision-induced dissociation) and much longer times (many seconds) in the FTMS experiments.¹⁴ From the data presented above, it would appear that the structures we observe at 200 ms should persist to much longer times. In the case of the +9 charge state, at least four conformations should be stable. Three should be stable for the +10 charge state. It is unlikely that the longer time ion trap and FTMS studies are sensitive to the transient +8(A, B and C) conformers.

ACKNOWLEDGMENT

This work is supported by a grant from the National Science Foundation (Grant CHE-0078737). E.R.B. is supported by a grant to the Indiana/Purdue University Indiana Instrumentation Institute (the III) from the Indiana 21st Century fund. The authors also acknowledge Anne E. Counterman for many helpful conversations regarding data analysis and interpretation.

(46) McLuckey, S. A.; Wells, J. M.; Stephenson, J. L.; Goeringer, D. E. *Int. J. Mass Spectrom.* **2000**, *200*, 137–161.

(47) Shvartsburg, A. A.; Jarrold, M. F. *Chem. Phys. Lett.* **1996**, *261*, 86–91.

(48) Mesleh, M. F.; Hunter, J. M.; Shvartsburg, A. A.; Schatz, G. C.; Jarrold, M. F. *J. Phys. Chem.* **1996**, *100*, 16082–16086.

Received for review July 3, 2001. Accepted October 3, 2001.

AC010744A